NANO LETTERS

2008
Vol. 8, No. 4
1142-1146

Carbon Nanotube−Polymer Nanocomposite Infrared Sensor

Basudev Pradhan,[†] Kristina Setyowati,[†] Haiying Liu,[‡] David H. Waldeck,[§] and Jian Chen*,[†]

Department of Chemistry and Biochemistry, University of Wisconsin−Milwaukee, Milwaukee, Wisconsin 53211, Department of Chemistry, Michigan Technology University, Houghton, Michigan 49931, and Department of Chemistry, University of Pittsburgh, Pittsburgh, Pennsylvania 15260

Received December 17, 2007; Revised Manuscript Received February 3, 2008

ABSTRACT

The infrared photoresponse in the electrical conductivity of single-walled carbon nanotubes (SWNTs) is dramatically enhanced by embedding SWNTs in an electrically and thermally insulating polymer matrix. The conductivity change in a 5 wt % SWNT−polycarbonate nanocomposite is significant (4.26%) and sharp upon infrared illumination in the air at room temperature. While the thermal effect predominates in the infrared photoresponse of a pure SWNT film, the photoeffect predominates in the infrared photoresponse of SWNT−polycarbonate nanocomposites.

Organic electronic materials offer ease of materials processing and integration, low cost, physical flexibility, and large device area as compared to traditional inorganic semiconductors.[1] Optoelectronic materials that are responsive at the wavelengths in the near-infrared (NIR) region (e.g., 800–2000 nm) are highly desirable for various demanding applications such as telecommunication, thermal imaging, remote sensing, thermal photovoltaics, and solar cells.[2] Organic photoconductive materials have yet to demonstrate sensitivity beyond ~800 nm.[2–4] Single-walled carbon nanotubes (SWNTs) have outstanding electronic and optical properties, which offer the possibility of a unified electronic and optoelectronic technology.[5,6] There are a number of reports on the infrared (IR) photoresponse in the electrical conductivity of individual SWNTs and SWNT films.[7–11] Avouris et al. measured the photoconductivity of individual SWNTs in a field-effect-transistor configuration upon IR laser illumination (10 W/mm^2), and the result was interpreted in a favor of the exciton model.[7,8] Levitsky et al. demonstrated that the arc-produced SWNT ($SWNT_{arc}$) film is capable of generating a very weak photocurrent upon continuous-wave IR illumination (12 mW/mm^2) in the air at room temperature, and the current increase upon IR illumination is only about 0.2%.[9] In addition, they observed a dark current drift due to oxygen adsorption and a relatively slow rise/decay (~4–5 s relaxation time) of the photocurrent in response to the on/off illumination.[9] Haddon et al. reported that the IR photoresponse in the electrical conductivity of a $SWNT_{arc}$ film is dramatically enhanced when the nanotube film is suspended in vacuum at low temperature.[11] For example, at 50 K, the $SWNT_{arc}$ film suspended in vacuum shows a resistance drop of 0.7% under an extremely low incident power of 0.12 μW of IR radiation. Their experimental data suggest that the IR photoresponse of the $SWNT_{arc}$ film arises mainly from the thermal effect. In other words, it is not the presence of photoexcited holes and electrons, but a rise in temperature and thermal carrier population, that is mainly responsible for the change in resistance of a SWNT $film_{arc}$.[11]

We report here that the IR photoresponse of SWNTs is dramatically improved by embedding SWNTs in an electrically and thermally insulating polymer matrix in the air at room temperature. In contrast to the gradual photoresponse and weak conductivity change (1.10%) observed in a HiPco-produced SWNT ($SWNT_{HiPco}$) film in the air at room temperature, the 5 wt % $SWNT_{HiPco}$−polycarbonate (PC) nanocomposite under the same IR illumination (power intensity: 7 mW/mm^2) shows a sharp photoresponse and strong conductivity change (4.26%). In fact, even the 1 wt % $SWNT_{HiPco}$−PC nanocomposite film shows a significant conductivity increase of 2.56% upon the same IR radiation, which outperforms the pure $SWNT_{HiPco}$ film (1.10% conductivity change) under the same conditions. While the thermal effect predominates in the IR photoresponse of the pure $SWNT_{HiPco}$ film, in our study and in Haddon et al.'s report. on the $SWNT_{arc}$ film,[11] we find that the photoexcitation effect predominates in the IR photoresponse of the 5 wt % $SWNT_{HiPco}$−PC nanocomposite.

* Corresponding author. E-mail: jianchen@uwm.edu.
† University of Wisconsin−Milwaukee.
‡ Michigan Technology University.
§ University of Pittsburgh.

10.1021/nl0732880 CCC: $40.75
Published on Web 03/12/2008

Table 1. IR Photoresponse in the Electrical Conductivity of $SWNT_{HiPco}$−PC Nanocomposite Films in the Air at Room Temperature[a]

p (wt %)	condition	σ_{dark} (S/cm)	$\Delta\sigma/\sigma_{dark}$ (%) IR_{total}	IR_{photo}	$IR_{thermal}$
1	undoped	5.1×10^{-2}	2.56	1.40	1.16
3	undoped	0.70	3.47	2.61	0.86
5	undoped	2.48	4.26	3.53	0.73
	I_2-doped	6.80	0.16	0.24	−0.08
100	undoped	150	1.10	0.06	1.04

[a] IR_{total} represents the overall conductivity change upon IR illumination (power intensity: 7 mW/mm^2). IR_{photo} represents the conductivity change due to the photo effect of the IR illumination. $IR_{thermal}$ represents the conductivity change due to the thermal effect of the IR illumination. p (wt %) represents the SWNT mass fraction.

We recently developed a versatile, nondamaging chemistry platform that enables us to engineer specific carbon nanotube (CNT) surface properties while preserving CNT's intrinsic properties.[12–17] We discovered that rigid, conjugated macromolecules, poly(*p*-phenylene ethynylene)s (PPEs), can be used to noncovalently functionalize and solubilize CNTs[12–14] and disperse CNTs uniformly in polymer matrices.[15–17] Purified $SWNTs_{HiPco}$ (Lot No. P0279) were purchased from Carbon Nanotechnologies, Inc., and were solubilized in chloroform with standard PPE along with vigorous shaking and/or short bath sonication.[12,13] The resulting $SWNT_{HiPco}$ solution was then mixed with a PC solution (for undoped samples) or a PC−iodine solution (for doped samples) in chloroform to produce a homogeneous $SWNT_{HiPco}$−PC composite solution, which was cast on a glass dish and dried very slowly to give a free-standing film after peeling from the substrate. Doped and undoped $SWNT_{HiPco}$−PC composites with various $SWNT_{HiPco}$ loadings were prepared according to the above procedure.[15–17] The pure $SWNT_{HiPco}$ film was obtained from the PTFE membrane after filtration of a suspension of $SWNTs_{HiPco}$ in chloroform. The typical film thickness was in the range 25–60 μm. The mass ratios of PPE:$SWNT_{HiPco}$ and iodine:$SWNT_{HiPco}$ were kept at 0.4 and 5, respectively. The $SWNT_{HiPco}$ loading values quoted in Table 1 are based on purified $SWNTs_{HiPco}$ only and exclude the PPE and iodine. The UV–vis-NIR absorption spectrum of the 5 wt % $SWNT_{HiPco}$−PC film on a quartz substrate was recorded with a Cary 5000 UV–vis-NIR spectrophotometer. Scanning electron microscopy (SEM) was performed using an Hitachi S-570 scanning electron microscope (accelerating voltage: 10 keV). No sample coating was used in the SEM experiment in order to avoid possible artifacts induced by the metal coating. The schematic device structure is shown in Figure 1a. The electrical contacts to the sample film were made with silver paste. The sample film was kept on a ceramic plate with proper thermal contact. The two-point probe electrical conductivity measurement was performed using a Keithley 2400 source meter instrument through the computer-controlled LabVIEW program. The IR light source was a xenon light bulb (XNiteFlashSTG, LDP LLC) with a long-pass NIR filter (X-Nite 1000 nm filter; 1000 nm cutoff at 50%; 1300 nm passband >90%). The incident power of the IR radiation was measured using a Newport power meter model 1918-C with an IR detector (918D-IR-OD3).

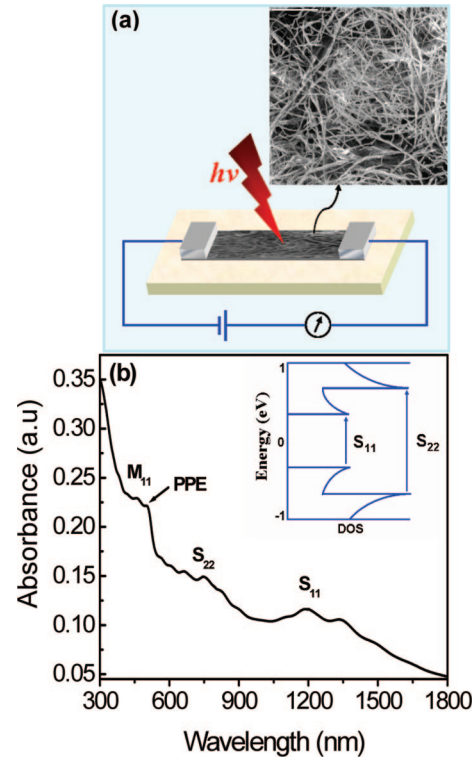

Figure 1. (a) Schematic experimental setup. Inset: SEM image of the 5 wt % $SWNT_{HiPco}$−PC nanocomposite film (scale bar: 1.0 μm). (b) UV–vis-NIR spectrum of the 5 wt % $SWNT_{HiPco}$−PC nanocomposite thin film. M_{11}, S_{11}, and S_{22} represent the band-gap transitions in metallic and semiconducting SWNTs. Inset: schematic energy band diagram of electron density of states (DOS) with interband transitions S_{11} and S_{22} in semiconducting SWNTs.

SEM shows the excellent dispersion of PPE−$SWNTs_{HiPco}$ in the PC matrix (Figure 1a), which is essential for obtaining composites with isotropic electrical conductivity. The UV–vis-NIR spectrum of the 5 wt % $SWNT_{HiPco}$−PC composite film shows the characteristic absorptions corresponding to the first (900–1600 nm) and second (600–900 nm) band-gap transitions of semiconducting $SWNTs_{HiPco}$ (Figure 1b).[18] The relatively weak absorptions corresponding to band-gap transitions of metallic $SWNTs_{HiPco}$ overlap with the broad and strong $\pi-\pi^*$ transition band (505 nm) of the planarized PPE.[13]

Figure 2a shows the typical photoresponse of the pure $SWNT_{HiPco}$ film upon the on/off IR illumination (power intensity: 7 mW/mm^2; on/off time period: 200 s) in the air at room temperature, which is qualitatively similar to that of the pure $SWNT_{arc}$ film.[9] It exhibits two notable features (Table 1 and Figure 2a): (1) relatively weak conductivity change (1.10%) upon IR illumination; (2) gradual rise and decay of the conductivity in response to the on/off IR illumination.

We found that the IR photoresponse in the electrical conductivity of SWNTs is dramatically enhanced by embedding the SWNTs in an insulating polymer matrix such as PC. As shown in Table 1, the 5 wt % $SWNT_{HiPco}$−PC nanocomposite demonstrates an overall conductivity change of 4.26% upon the on/off IR illumination (power intensity: 7 mW/mm^2; on/off time period: 30 s) in the air at room

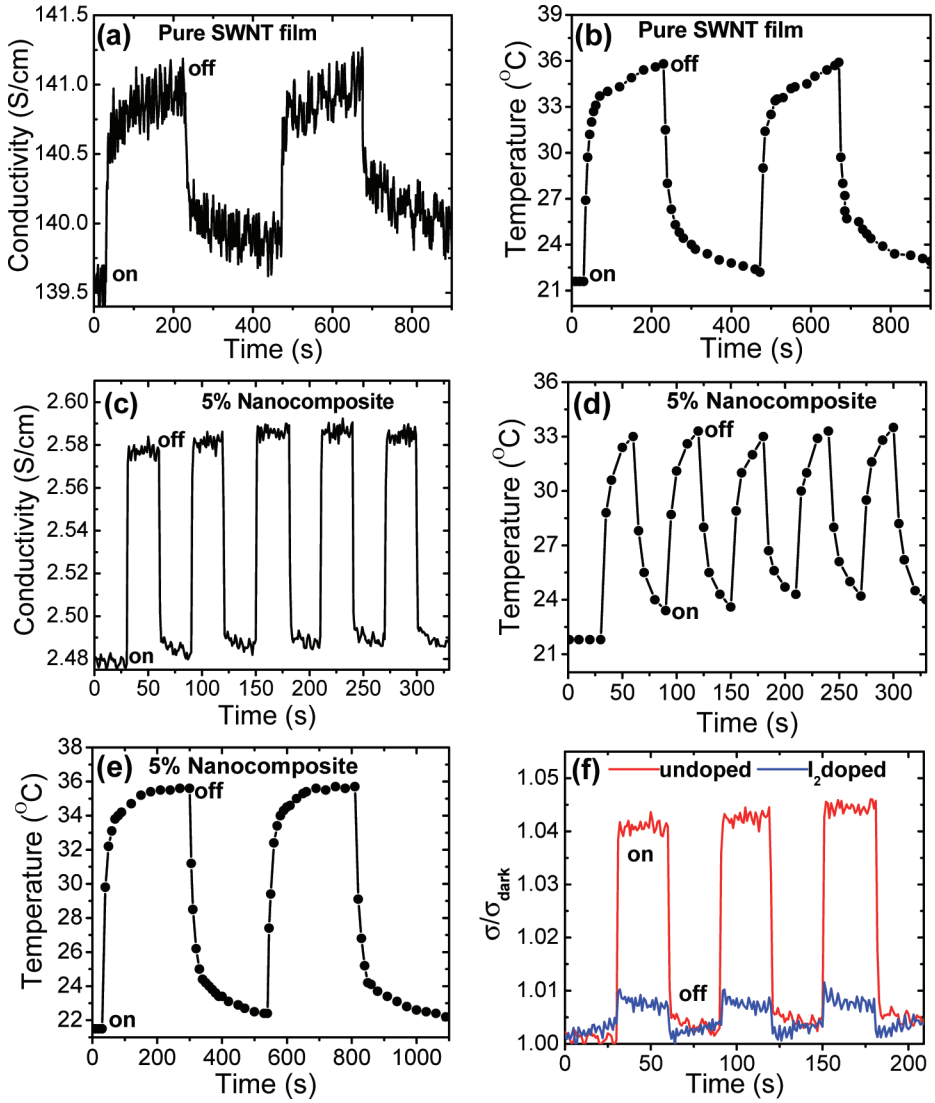

Figure 2. Conductivity response of (a) the pure $SWNT_{HiPco}$ film and (c) the 5 wt % $SWNT_{HiPco}$−PC nanocomposite film to the on/off IR illumination (power intensity: 7 mW/mm^2). Temperature response of (b) the pure $SWNT_{HiPco}$ film and (d) the 5 wt % $SWNT_{HiPco}$−PC nanocomposite film to the same on/off IR illumination. (e) Temperature response of the $SWNT_{HiPco}$−PC nanocomposite film to the same IR illumination with longer on/off time period. (f) Relative conductivity (σ/σ_{dark}) response of the undoped and I_2-doped 5 wt % $SWNT_{HiPco}$−PC nanocomposite film to the same on/off IR illumination.

temperature, which is nearly 4 times of that (1.10%) observed in the pure $SWNT_{HiPco}$ film under the same condition, 21 times of that (0.2%) observed in the pure $SWNT_{arc}$ film in the air at room temperature (12 mW/mm^2),[9] and 6 times of that (0.7%) observed in the pure $SWNT_{arc}$ film in the vacuum at 50 K.[11] Furthermore, the conductivity change in the $SWNT_{HiPco}$−PC nanocomposite becomes sharp in response to the on/off IR illumination (Figure 2c).

According to recent studies, the photoexcitation of semiconducting SWNTs with IR light leads to generation of excitons instead of free carriers.[6,7,19–21] The IR light could have two main effects on the conductivity of SWNTs: (1) Photo effect: the excitons can be dissociated into free electrons and holes thermally or by a large electric field,[11,21,22] which increases the conductivity of SWNTs. (2) Thermal effect: the excitons decay into heat and the strong warming of SWNT reduces its resistance.[11]

In order to estimate the thermal effect contribution ($IR_{thermal}$) to the overall conductivity change (IR_{total}), we measured the temperature response to the on/off IR illumination (power intensity: 7 mW/mm^2) in the pure $SWNT_{HiPco}$ film and $SWNT_{HiPco}$−PC nanocomposite films. The temperature of the pure $SWNT_{HiPco}$ film increases to ~36 °C upon 200 s of IR illumination (Figure 2b), while the temperature of the 5 wt % $SWNT_{HiPco}$−PC nanocomposite increases to ~33 °C upon 30 s of IR illumination (Figure 2d). Interestingly, the pattern of conductivity response (Figure 2a) is very similar to that of temperature response (Figure 2b) in the pure $SWNT_{HiPco}$ film, whereas the pattern of conductivity response (Figure 2c) is dramatically different from that of temperature response (Figure 2d) in the 5 wt % $SWNT_{HiPco}$−PC nanocomposite. In addition, Figure 2e shows that the temperature of the 5 wt % $SWNT_{HiPco}$−PC nanocomposite reaches the equilibrium temperature ~35.5 °C upon 150 s

of IR illumination, which provides the upper limit of the temperature increase in the 5 wt % $SWNT_{HiPco}$−PC nanocomposite caused by the IR heating effect. The conductivity change owing to the sample temperature change ($IR_{thermal}$) can be calculated on the basis of the temperature dependence of conductivity data of the samples (Supporting Information).[17] The conductivity change due to the photo effect (IR_{photo}) can be calculated on the basis of the equation $IR_{total} = IR_{thermal} + IR_{photo}$. The IR_{photo} and $IR_{thermal}$ data are included in Table 1. The $IR_{thermal}/IR_{total}$ is about 95% for the pure $SWNT_{HiPco}$ film, indicating that the thermal effect predominates in the IR photoresponse of the pure $SWNT_{HiPco}$ film (Figure 2a and Table 1), which is in agreement with the literature result.[11] In contrast, the $IR_{thermal}/IR_{total}$ is only about 17% for the 5 wt % $SWNT_{HiPco}$−PC nanocomposite, suggesting that the photo effect, rather than the thermal effect, predominates in the IR photoresponse of the 5 wt % $SWNT_{HiPco}$−PC nanocomposite (Figure 2c and Table 1). This also explains why the conductivity change in 5 wt % $SWNT_{HiPco}$−PC nanocomposite is sharp upon the on/off IR illumination, whereas the rise and decay of the conductivity in pure $SWNT_{HiPco}$ film is gradual in response to the on/off IR illumination.

The p-type doping of SWNTs by iodine creates charge carriers in SWNT walls and, as a result, the semiconducting SWNTs become metallic, while metallic SWNTs become even more conducting due to the increased density of charge carriers.[17] As a result, the conductivity change of the iodine-doped 5 wt % $SWNT_{HiPco}$−PC nanocomposite is very weak (0.16%) upon IR illumination (Table 1 and Figure 2f). This experiment shows that semiconducting SWNTs are critical to the IR photoresponse of nanotube materials.

The dependence of the photocurrent on the incident IR light intensity demonstrates a linear relationship as expected (Figure 3a). The 5 wt % $SWNT_{HiPco}$−PC composite film shows a detectable IR photoresponse at a light intensity as low as 0.7 mW/mm^2 (Figure 3a). Figure 3b shows that the IR photoresponse time of the 5 wt % $SWNT_{HiPco}$−PC composite film nanocomposite film is about 60 ms, which is most likely determined by the electrically insulating PC polymer layer between adjacent $SWNTs_{HiPco}$,[17,23] which acts as a potential barrier to internanotube hopping.

Most interestingly, our experimental data suggest that the electrically and thermally insulating PC matrix (electrical conductivity: 10^{-15} S/cm; thermal conductivity: 0.2 W/(m K)) may have a significant impact on the IR photoresponse mechanism of $SWNT_{HiPco}$−PC nanocomposites. While the thermal effect predominates in the IR photoresponse of the pure $SWNT_{HiPco}$ film, the photo effect predominates in the IR photoresponse of the 5 wt % $SWNT_{HiPco}$−PC nanocomposite (Table 1). The PC matrix may promote the exciton dissociation via two possible mechanisms: (1) The local temperature of SWNTs embedded in the thermally insulating PC matrix can be significantly increased upon IR illumination, providing sufficient thermal energy required for the exciton dissociation.[22] (2) In SWNT−PC composites, the SWNTs are coated with an electrically insulating PC thin layer,[23] which acts as a potential barrier to internanotube hopping.[17,24–26] The

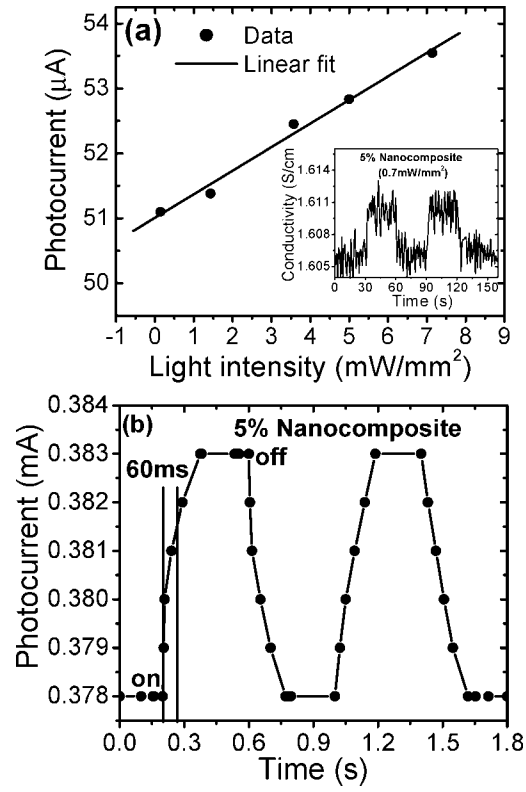

Figure 3. (a) Dependence of photocurrent of the 5 wt % $SWNT_{HiPco}$−PC nanocomposite on the IR light intensity. Inset: conductivity response of the 5 wt % $SWNT_{HiPco}$−PC nanocomposite film to the on/off IR illumination at 0.7 mW/mm^2 light intensity. (b) Photocurrent response of the 5 wt % $SWNT_{HiPco}$−PC nanocomposite film to the on/off IR illumination (power intensity: 7 mW/mm^2).

enhanced local electric field at the SWNT−PC interface could help the exciton dissociation.[21]

Previous studies showed that the electric field at the CNT−conjugated polymer interface is mainly responsible for the enhanced dissociation of excitons generated in conjugated polymers (e.g., polythiophene) by visible light,[27–29] which lend further support for one of our proposed mechanisms that the enhanced local electric field at the SWNT−insulating polymer interface could help the dissociation of excitons generated in semiconducting SWNTs by the near-IR light. The comparison of UV–vis-NIR spectra of pristine $SWNT_{HiPco}$ (Supporting Information) and $SWNT_{HiPco}$−PC (Figure 1b) films indicates that the dramatically enhanced IR photoresponse observed in the $SWNT_{HiPco}$−PC nanocomposite film cannot be attributed primarily to the potential nanotube debundling effect.

The 3D SWNT network is also crucial to the fast conduction of free carriers produced by the exciton dissociation. The 5 wt % $SWNT_{HiPco}$−PC nanocomposite can conduct the free carriers better than the 3 and 1 wt % nanocomposites; therefore, the IR_{photo} is more significant than $IR_{thermal}$ in 5 wt % nanocomposite as compared to 3 and 1 wt % nanocomposites (Table 1).

In conclusion, we demonstrate that the IR photoresponse in the electrical conductivity of SWNTs is dramatically enhanced by embedding the SWNTs in an insulating polymer

matrix such as PC in the air at room temperature. We show that semiconducting SWNTs are critical to the IR photoresponse of nanotube materials. Our experimental data also suggest that the electrically and thermally insulating polymer matrix may have a significant impact on the IR photoresponse mechanism of SWNT−polymer nanocomposites. While the thermal effect predominates in the IR photoresponse of the pure $SWNT_{HiPco}$ film, the photo effect predominates in the IR photoresponse of $SWNT_{HiPco}$−PC nanocomposites.

Acknowledgment. J.C. thanks the financial support from the National Science Foundation (DMI-06200338), UWM start-up fund, and UWM Research Growth Initiative award.

Supporting Information Available: Temperature dependences of relative conductivity σ_T/σ_{RT} of the pure $SWNT_{HiPco}$ film and $SWNT_{HiPco}$−PC nanocomposites; UV–vis-NIR spectrum of pristine $SWNT_{HiPco}$ film. This material is available free of charge via the Internet at http://pubs.acs.org.

References

(1) Forrest, S. R. *Nature (London)* **2004**, *428*, 911–918.
(2) McDonald, S. A.; Konstantatos, G.; Zhang, S.; Cyr, P. W.; Klem, E. J. D.; Levina, L.; Sargent, E. H. *Nat. Mater.* **2005**, *4*, 138–142.
(3) Yoshino, K.; Lee, S.; Fujii, A.; Nakayama, H.; Schneider, W.; Naka, A.; Ishikawa, M. *Adv. Mater.* **1999**, *11*, 1382–1385.
(4) Brabec, C. J.; Winder, C.; Sariciftci, N. S.; Hummelen, J. C.; Dhanabalan, A.; van Hal, P. A.; Janssen, R. A. J. *Adv. Funct. Mater.* **2002**, *12*, 709–712.
(5) Avouris, Ph.; Chen, J.; Freitag, M.; Perebeinos, V.; Tsang, J. C. *Phys. Status Solidi B* **2006**, *243*, 3197–3203.
(6) Avouris, Ph.; Chen, Z.; Perebeinos, V. *Nat. Nanotechnol.* **2007**, *2*, 605–615.
(7) Freitag, M.; Martin, Y.; Misewich, J. A.; Martel, R.; Avouris, Ph. *Nano Lett.* **2003**, *3*, 1067–1071.
(8) Qiu, X.; Freitag, M.; Perebeinos, V.; Avouris, Ph. *Nano Lett.* **2005**, *5*, 749–752.
(9) Levitsky, A.; Euler, W. B. *Appl. Phys. Lett.* **2003**, *83*, 1857–1859.
(10) Fujiwara, A.; Matsuoka, Y.; Matsuoka, Y.; Suematsu, H.; Ogawa, N.; Miyano, K.; Kataura, H.; Maniwa, Y.; Suzuki, S.; Achiba, Y. *Carbon* **2004**, *42*, 919–922.
(11) Itkis, M. E.; Borondics, F.; Yu, A.; Haddon, R. C. *Science* **2006**, *312*, 413–416.
(12) Chen, J.; Liu, H.; Weimer, W. A.; Halls, M. D.; Waldeck, D. H.; Walker, G. C. *J. Am. Chem. Soc.* **2002**, *124*, 9034–9035.
(13) Chen, J.; Ramasubramaniam, R.; Liu, H. *Mater. Res. Soc. Symp. Proc.* **2005**, *858E*, HH 12.4.
(14) Chen, J.; Xue, C.; Ramasubramaniam, R.; Liu, H. *Carbon* **2006**, *44*, 2142–2146.
(15) Ramasubramaniam, R.; Chen, J.; Liu, H. *Appl. Phys. Lett.* **2003**, *83*, 2928–2930.
(16) Chen, J.; Ramasubramaniam, R.; Xue, C.; Liu, H. *Adv. Funct. Mater.* **2006**, *16*, 114–119.
(17) Sankapal, B.; Setyowati, K.; Chen, J.; Liu, H. *Appl. Phys. Lett.* **2007**, *91*, 173103.
(18) Hamon, M. A.; Itkis, M. E.; Niyogi, S.; Alvaraez, T.; Kuper, C.; Menon, M.; Haddon, R. C. *J. Am. Chem. Soc.* **2001**, *123*, 11292–11293.
(19) Spataru, C. D.; Ismail-Beigi, S.; Benedict, L. X.; Louie, S. G. *Phys. Rev. Lett.* **2004**, *92*, 077402.
(20) Perebeinos, V.; Tersoff, J.; Avouris, P. *Phys. Rev. Lett.* **2004**, *92*, 257402.
(21) Wang, F.; Dukovic, G.; Brus, L. E.; Heinz, T. *Science* **2005**, *308*, 838–841.
(22) Matsuoka, Y.; Fujiwara, A.; Ogawa, N.; Miyano, K.; Kataura, H.; Maniwa, Y.; Suzuki, S.; Achiba, Y. *Sci. Technol. Adv. Mater.* **2003**, *4*, 47–50.
(23) Ding, W.; Eitan, A.; Fisher, F. T.; Chen, X.; Dikin, D. A.; Andrews, R.; Brinson, L. C.; Schadler, L. S.; Ruoff, R. S. *Nano Lett.* **2003**, *3*, 1593–1597.
(24) Kilbride, B. E.; Coleman, J. N.; Fraysse, J.; Fournet, P.; Cadek, M.; Drury, A.; Hutzler, S.; Roth, S.; Blau, W. J. *J. Appl. Phys.* **2002**, *92*, 4024–4030.
(25) Barrau, S.; Demont, P.; Peigney, A.; Laurent, C.; Lacabanne, C. *Macromolecules* **2003**, *36*, 5187–5194.
(26) Sichel, E. K.; Gittleman, J. I.; Sheng, P. *Phys. Rev. B* **1978**, *18*, 5712–5716.
(27) Kymakis, E.; Amaratunga, G. A. J. *Appl. Phys. Lett.* **2002**, *80*, 112–114.
(28) Xu, Z.; Wu, Y.; Hua, B.; Ivanov, I. N.; Geohegan, D. B. *Appl. Phys. Lett.* **2005**, *87*, 263118.
(29) Pradhan, B.; Batabyal, S. K.; Pal, A. J. *Appl. Phys. Lett.* **2006**, *88*, 093106.

NL0732880